

# Interplay between scintillation and ionization in liquid xenon Dark Matter searches

Fedor Bezrukov<sup>a,b,1</sup>, Felix Kahlhoefer<sup>a</sup>, Manfred Lindner<sup>a</sup>

<sup>a</sup>Max-Planck-Institut für Kernphysik, Postfach 103980, D-69029 Heidelberg, Germany

<sup>b</sup>Theoretische Teilchenphysik, Ludwig-Maximilians-Universität München, Theresienstr. 37, 80333 München, Germany

---

## Abstract

We calculate the relative scintillation efficiency  $\mathcal{L}_{\text{eff}}$  in liquid xenon. Using a simple estimate for the electronic and nuclear stopping powers together with an analysis of recombination processes we predict *both* the ionization and the scintillation yields. We argue that using more reliable data on the ionization yield it is possible to verify our assumptions on the atomic cross sections and to predict the value of  $\mathcal{L}_{\text{eff}}$ . From the presently available data for the ionization yield, we conclude that the scintillation yield does not decrease at low nuclear recoil energies, which has important consequences for the robustness of bounds for low WIMP masses in liquid xenon Dark Matter searches.

*Keywords:* Dark Matter search, liquid xenon, WIMP, relative scintillation efficiency

---

## 1. Introduction

The recent results of XENON100 [1] correspond to a major increase of sensitivity for the Dark Matter (DM) searches and further improvements are expected soon when more data will be released. However, the analysis of the detector properties turns out to be subtle for low recoil energies, corresponding to low mass DM particles (below 10 GeV). The interest in this parameter region is additionally heated by claims of DM observation [2, 3]. The problem is the proper reconstruction of the nuclear recoil energy from the primary scintillation signal (S1) in liquid xenon in the limit of low recoil energies. Direct experimental calibration is rather difficult for low nuclear recoil energy and is prone to large systematic uncertainties, which led to mutually contradicting experimental measurements below 10 keV [4–11] (see figure 4b).

A theoretical treatment of the problem requires the determination of the scintillation yield for a slow moving xenon atom. The task can be roughly divided into three parts: the problem of ionization and excitation probabilities in the individual collisions of xenon atoms, the problem of simulating the propagation through the media, and finally the problem of possible recombination of the produced free electrons and ions. The outcome of such a theoretical treatment would be predictions for *both* the scintillation and the ionization signals produced in the detector.

At sufficiently high energies the total electronic excitations in the atomic collisions can be reasonably well described by Lindhard's theory [12]. It approximates the

process by point-like interactions between the incoming nucleus and electrons in the electron cloud of the target, and is applicable for the case of nuclear recoil velocity  $v_{\text{nr}} \approx v_0 = e^2/\hbar$  (or  $E_{\text{nr}} \approx 1$  MeV). However, for smaller energies, the individual collisions are much harder to calculate and require a nonperturbative analysis of the electronic movement [13]. For this reason, it is very difficult to describe inelastic collisions at energies much below 100 keV.

In this article we do not attempt to make an ab-initio theoretical calculation of all the above processes, which is a very difficult task. Instead we make use of theoretical connections between the scintillation and ionization yields and the fact that the ionization yield is measured more reliably at low nuclear recoil energies, than the scintillation yield [6] (see figure 4a). Therefore we parameterize the unknown cross sections in order to compare the resulting scintillation and ionization yields with experimental data. From the data for the ionization yield we conclude that we can not obtain cross sections leading to small electron excitations at small recoil energies without spoiling the fit of the ionization yield in figure 4a. This observation leads to the prediction that the scintillation yield also can not decrease much at small nuclear recoil energies.

The paper is organized as follows: in section 2 we review the process of generation of scintillation light and ionization in liquid xenon. Section 3 introduces the notion of the nuclear and electronic stopping powers, which correspond to the analysis of individual xenon scattering events. Moreover, we calculate the total energy in the electronic excitations, and then analyze the recombination process in section 4. In section 5 all the results are collected and translated into the ionization and scintillation yields and compared with the experimental data. Section 6 contains

---

*Email addresses:* Fedor.Bezrukov@physik.uni-muenchen.de (Fedor Bezrukov), Felix.Kahlhoefer@mpi-hd.mpg.de (Felix Kahlhoefer), Lindner@mpi-hd.mpg.de (Manfred Lindner)

<sup>1</sup>ASC Preprint Number: LMU-ASC 82/10

our conclusions and further prospects.

## 2. Production of scintillation light in liquid xenon

A large variety of effects must be taken into account to describe all physical processes that lead from the initial recoil to the production of scintillation light in liquid xenon. Specifically, we expect the following steps [14]:

- In a WIMP-like scattering event, an energy of 1–100 keV is transferred to the nucleus.<sup>2</sup> As the corresponding recoil velocity is well below the Fermi velocity of the most loosely bound electrons, we expect the atom to remain neutral in the scattering process.
- The recoiling atom will scatter off neighboring nuclei. While most scattering events are expected to be elastic, there will occasionally be inelastic collisions leading to excitation or ionization of either (or both) of the atoms.
- After each scattering process both atoms will continue their propagation with a fraction of the initial recoil energy. Consequently, both can again scatter elastically or inelastically off other atoms.
- During the process of thermalization the recoiling xenon atoms will leave behind a large number of ionized or excited xenon atoms — distributed along many branches of the initial track.
- The free electrons will now either recombine with surrounding ions to form excited xenon atoms or escape from recombination. The fraction of escaping electrons will depend on the strength of the applied electric drift field, but some electrons will escape even in the absence of a field.
- Excited xenon atoms are free initially, but will soon be self-trapped and form excimers. These excimers emit vuv scintillation light on the transition to the ground state. In a simplified picture, the process is



- In some cases, especially at high excitation density, two excited xenon atoms will combine to produce only one scintillation photon. This process, known as biexcitonic quenching, will effectively reduce the scintillation yield.

<sup>2</sup>Note that in the context of liquid noble gas detectors nuclear recoil energies are often quoted in keV<sub>nr</sub>. This unit is chosen to emphasize that any energy reconstructed from an S1 signal depends on the effective scintillation yield (and is therefore not necessarily physical). Since we are concerned with actual physical processes and not the detector signals in this paper, we will give nuclear recoil energies in keV.

At first sight, the large number of steps seems to make it very hard to disentangle possible ambiguities. A decrease of scintillation efficiency at low recoil energies could, for example, be equally attributed to a decreasing cross section for inelastic scattering (for example due to threshold effects), a different track structure, an increasing fraction of escaping electrons or a stronger quenching mechanism. This ambiguity can be lifted at least partially by considering not only the effective scintillation yield of nuclear recoils, but also the ionization yield. This quantity is much better measured (because free electrons can be extracted with high efficiency and the signal can be strongly amplified in the gas phase), but has been — to the best of our knowledge — ignored in all previous attempts to give a theoretical model for the scattering process in liquid xenon.

The sum of ionization and scintillation, which we will refer to as the total electronic excitation, should correspond to the total energy lost in inelastic collisions. Consequently, it should only depend on the scattering cross sections and not on the processes occurring later, such as recombination, which will only lead to a redistribution between ionization and scintillation. Thus, if both signals showed a similar energy dependence, this would suggest a general suppression of inelastic scattering at low energies — which is what one might naively expect. However, a strong increase of the ionization yield at low energies is actually observed experimentally. This observation indicates that the suppression of the scintillation signal at low energies does not result from the actual inelastic scattering processes, but from the large number of escaping electrons.

The effective scintillation yield of nuclear recoils is usually described by the dimensionless quantity  $\mathcal{L}_{\text{eff}}$ , called relative scintillation efficiency. It relates the S1 scintillation signal to the physical recoil energy of the nucleus  $E_{\text{nr}}$  as

$$E_{\text{nr}} = \frac{S1}{L_y \cdot \mathcal{L}_{\text{eff}}} \cdot \frac{S_e}{S_n} \quad (3)$$

$L_y$  is the light yield for 122 keV electron recoils and  $S_{e,n}$  are the electric field quenching factors for electronic and nuclear recoils. Thus,  $\mathcal{L}_{\text{eff}}$  quantifies the suppression of scintillation for nuclear recoils compared to 122 keV electron recoils at zero electric field.

## 3. Stopping powers of liquid xenon

In this section we will describe the interactions of neutral xenon atoms and discuss possible scattering processes at energies of a few keV. The quantities we are interested in are the rate at which energy is transferred to recoiling nuclei by elastic collisions and the rate at which electrons are excited by inelastic collisions. These quantities are often called nuclear stopping power and electronic stopping power.

### 3.1. Electronic stopping power

The electronic stopping power is defined as the average energy which an atom loses to electronic excitations per distance travelled through the detector,  $(dE/dx)_e$ . In a “semiclassical” approach, an electron is excited when it collides with a nucleus. The stopping power should therefore be proportional to the electron mass density  $n_0$ , their velocity  $v_F$ , the momentum transfer cross section  $\sigma_{tr}(v_F)$ , and the velocity of the incoming particle  $v$ . In fact, electronic stopping is often described by [15–19]

$$\left(\frac{dE}{dx}\right)_e = n_0 v v_F \sigma_{tr}(v_F). \quad (4)$$

We should take a moment to discuss the validity of such a semiclassical approach. Equation (4) is in fact based on several assumptions:

- Instead of describing the atomic system by a many-particle wavefunction, we claim that only the electron density is relevant to the problem, *and* we ignore the modification of the electron density during the atomic collision.
- Collisions between electrons and nuclei are treated like classical point like interactions.
- Electrons are assumed to be free. Consequently, no minimal energy transfer is required for an excitation.

For a uniform electron gas the electronic stopping power is proportional to the velocity of the incoming particle, a result that has been derived in [12]. The authors obtain

$$\left(\frac{dE}{dx}\right)_e = \sqrt{8}\pi e^2 a_0 \zeta_0 Z N \cdot \frac{v}{v_0}, \quad (5)$$

where  $a_0$  and  $v_0$  are Bohr radius and Bohr velocity respectively and  $\zeta_0$  is an empirical parameter, often<sup>3</sup> set to  $\zeta_0 = Z^{1/6}$ .  $N = 13.76 \text{ nm}^{-3}$  is the number density of xenon atoms. This formula should also be valid for nuclear velocities  $v < v_0$ .

However, there is no reason that we can extrapolate the velocity proportional behavior all the way down to  $v = 0$ . In fact, at very low velocities, departures from velocity-proportionality have been observed experimentally [16]. Moreover, there are several theoretical arguments in favor of a more rapid drop of  $(dE/dx)_e$  for  $v < v_0$ . The two most important ones are threshold effects and Coulomb effects.

The argument for threshold effects essentially goes as follows: in an elastic collision between a nucleus and a free electron, only a fraction  $m_e/m_N$  of the nucleus energy can be transferred to the electron. For nuclei with energies in the keV range, the resulting electron energy is at most a

<sup>3</sup>In an independent derivation, Firsov [20] obtained the same formula with  $\zeta_0 \approx 1.63$ .

few eV — so we can no longer ignore gap energies or the work function of xenon. There has been a long and intense discussion on whether such threshold effects are present or not (see for example [21]). However, many experiments and theoretical considerations report electronic excitations far below the naive threshold [13, 22].

An effect from Coulomb repulsion is expected, because at very low relative velocities colliding nuclei will not penetrate the electron clouds of each other strongly. Consequently, with decreasing energy the recoiling nucleus will probe only regions of lower electron density [23].

Both these arguments fail, because they continue to exploit the point-like interaction of the nucleus with the electron. However, for low nuclear velocity the electron clouds rearrange during the collision (or, in a more semiclassical language, the electron makes several rotations in the combined electric field of the two colliding atoms during the collision). This effect leads to a much more complicated non-perturbative mechanism of the energy transfer to the electron. For an analysis of such collisions in the case of simple atoms, we refer to [13].

Ideally, exact or approximate quantum mechanical calculations for the Xe–Xe scattering process must be performed. Lacking such calculations, we will continue to use equation (5) even for low energies. However, we will eventually parameterize our ignorance of the cross section by introducing some suppression factor

$$\left(\frac{dE}{dx}\right)_e \rightarrow F(v/v_0) \left(\frac{dE}{dx}\right)_e, \quad (6)$$

and then compare with the experimental data on ionization and scintillation for various suppression factors.

To conclude this section, we provide dimensionless quantities instead of  $(dE/dx)_e$ , which are usually preferred in the literature. Therefore, we define

$$\epsilon = \frac{a}{2e^2 Z^2} E \quad (7)$$

$$\rho = N\pi a^2 x \quad (8)$$

$$s_e = \frac{d\epsilon}{d\rho} = \frac{(dE/dx)_e}{2\pi e^2 a Z^2 N} = \frac{a_0 \zeta_0}{a} \sqrt{\frac{8\epsilon}{e^2 a m_N}}, \quad (9)$$

where  $a = 0.626 a_0 Z^{-1/3}$  is the Thomas-Fermi screening length. For liquid xenon, the reduced energy  $\epsilon$ , which we will use throughout the rest of the paper, can be expressed as  $\epsilon = 1.05 \cdot 10^{-3} E_{nr} / \text{keV}$ .

### 3.2. Nuclear stopping power

The second quantity needed to calculate the amount of energy lost to electronic excitations is the nuclear stopping power, corresponding to the probability for elastic scattering of two xenon atoms. To calculate the cross section, we approximate the electron wave functions by the electron density, and ignore modifications of the electron clouds during the collision. The energy transfer in such a collision depends in general on the energy  $E_{nr}$  of the projectile and the scattering angle  $\theta$ . However, it turns out that due

to scaling properties all relevant functions depend only on the combined variable [24]

$$\eta = \epsilon \sin \frac{\theta}{2}, \quad (10)$$

where  $\epsilon$  again denotes the reduced energy.

The differential cross section for elastic scattering can then be written as

$$\frac{d\sigma}{d\eta} = \pi a^2 \frac{f(\eta)}{\eta^2}, \quad (11)$$

where  $a$  is again the screening radius. The function  $f(\eta)$  depends on the screening function that we adopt to describe the charge density. For a large number of screening functions,  $f(\eta)$  can approximately be written as [25]

$$f(\eta) \approx \frac{\lambda \eta^{1-2m}}{(1 + [2\lambda \eta^{2(1-m)}]^q)^{1/q}}. \quad (12)$$

From  $f(\eta)$  we can obtain the dimensionless nuclear stopping power  $s_n(\epsilon)$ :

$$s_n(\epsilon) = \frac{1}{\epsilon} \int_0^\epsilon d\eta f(\eta). \quad (13)$$

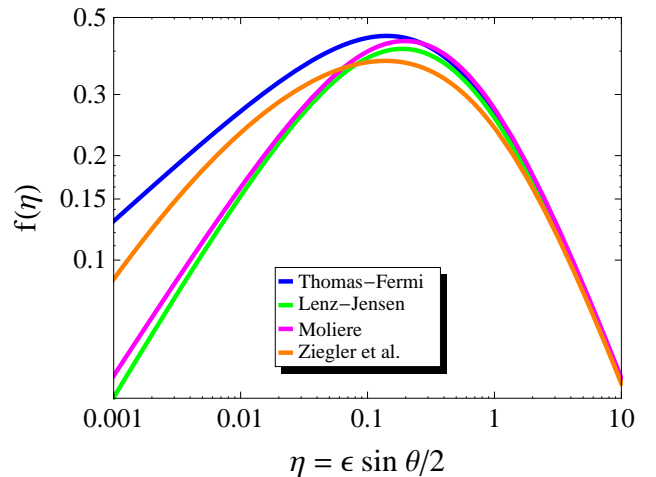
Both quantities,  $f(\eta)$  and  $s_n(\epsilon)$  have been calculated by various authors with differing results. The large uncertainties, especially for the low energy region, are due to different approximations for the screening function. Lindhard et al. favor the Thomas-Fermi screening function corresponding to  $m = 0.333$ ,  $q = 0.667$ ,  $\lambda = 1.309$ . However, today it is generally agreed that the Thomas-Fermi screening function overestimates the potential at large distances and therefore gives too large stopping powers at low energies [24]. One therefore often prefers the Molière or the Lenz-Jensen screening functions that show better agreement with experimental data. They correspond to the parameter choices  $m = 0.216$ ,  $q = 0.570$ ,  $\lambda = 2.37$  and  $m = 0.191$ ,  $q = 0.512$ ,  $\lambda = 2.92$ , respectively. For a comparison of the different screening functions, see figure 1.

Ziegler et al. [26] have confronted the different screening functions with experimental data and numerical results from Hartree-Fock methods. They find yet another (so-called universal) screening function given by the following expression:<sup>4</sup>

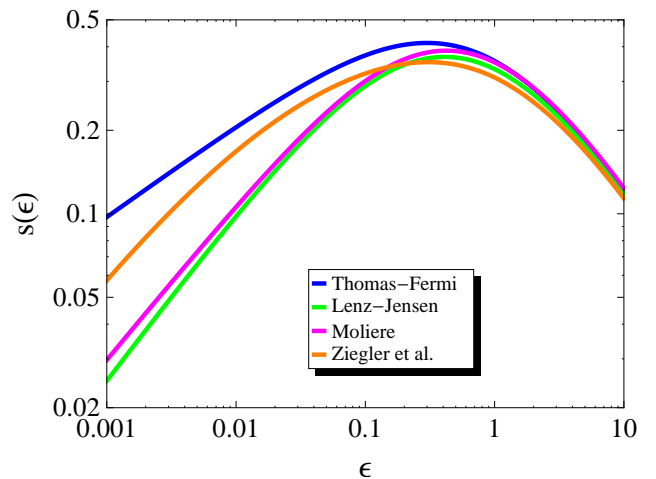
$$s_n(\epsilon_Z) = \frac{\ln(1 + 1.1383\epsilon_Z)}{2[\epsilon_Z + 0.01321\epsilon_Z^{0.21226} + 0.19593\epsilon_Z^{0.5}]}. \quad (14)$$

From this,  $f(\eta)$  can be calculated using  $f(x) = \frac{d}{dx} [xs(x)]$ .

<sup>4</sup>It is important to notice that Ziegler et al. use a slightly different definition for the reduced energy, because they assume a different screening length. For xenon, the conversion factor is  $\epsilon_Z = 1.068\epsilon$ .



(a) Screening function



(b) Nuclear stopping power

Figure 1: Comparison of different choices for the the nuclear stopping power.

While the universal screening function from Ziegler et al. appears to be the most reliable, the advantage of the simpler screening functions is that  $f(\eta)$  can be approximated by a power law for very small values of  $\eta$  (i.e.  $\eta < 10^{-4}$ ):

$$f(\eta) \simeq \lambda \eta^{1-2m}. \quad (15)$$

In the following we will use the universal screening function unless stated otherwise.

### 3.3. Total electronic excitation

In this section we will combine the the nuclear stopping power  $s_n(\epsilon)$  from equation (14) and the electronic stopping power  $s_e(\epsilon)$  from equation (4) in order to predict what amount of the initial recoil energy is transferred to electronic excitations. We will denote the total energy in

electronic excitations by  $\kappa(\epsilon)$  and also define the quotient

$$\xi(\epsilon) = \frac{s_e(\epsilon)}{s_n(\epsilon)}. \quad (16)$$

First of all we should try to discuss the general trends which we expect for  $\kappa(\epsilon)$  and  $\xi(\epsilon)$ . At energies above one MeV, inelastic collisions will dominate because the electronic stopping power grows proportional to  $\sqrt{E}$ , while the nuclear stopping power decreases after reaching its maximum around 100 keV. Consequently,  $\kappa(\epsilon) \approx \epsilon$  in this energy region. At energies of a few keV and below, the nuclear stopping power is much larger than the electronic stopping power. Consequently, we expect  $\kappa(\epsilon) \ll \epsilon$  and  $\xi(\epsilon) \ll 1$ .

In the low energy region, a first estimate for  $\kappa(\epsilon)$  is given by

$$\kappa(\epsilon) = \frac{\epsilon \cdot s_e(\epsilon)}{s_n(\epsilon) + s_e(\epsilon)} \approx \epsilon \cdot \xi(\epsilon). \quad (17)$$

Making this estimate, we have included only electronic excitations produced by the primary recoiling nucleus. We expect, however, that at least some recoiling nuclei from secondary elastic collisions still have enough energy to inelastically excite other atoms. Thus, part of the energy lost in elastic collisions can still be transferred into electronic excitations.

To take this effect into account, we could try to perform numerical simulations. However, in [27], Lindhard et al. have derived an integral equation to determine  $\kappa(\epsilon)$ . Under the approximation that most electronic excitations occur at large impact parameter and have only small energy transfer, the authors show that for  $\xi(\epsilon) \ll 1$ ,  $\kappa(\epsilon) \propto \epsilon \cdot \xi(\epsilon)$ . The constant of proportionality can be calculated analytically, if  $\xi(\epsilon)$  can be described by a power law. Here, we do not want to restrict ourselves to this case, so we will keep the constant of proportionality as a free parameter, writing

$$\kappa(\epsilon) = \alpha \epsilon \xi(\epsilon). \quad (18)$$

For  $\alpha = 1$  we recover the simple estimate in equation (17) which is supposed to underestimate  $\kappa$ , so we expect  $\alpha > 1$ , but still of order 1, for consistency.

For Thomas-Fermi screening, we obtain from equation (15) that  $\xi(\epsilon) \propto \epsilon^{0.17}$  and therefore  $\kappa(\epsilon) \propto \epsilon^{1.17}$ . Consequently, Lindhard's theory predicts an increasing  $\xi(\epsilon)$  as the nuclear recoil energy increases from 1 keV to 100 keV. This result has often been quoted as a possible explanation for the energy dependence of the scintillation yield in liquid xenon. However, we understand now that this result strongly depends on our choice for the nuclear stopping power. As argued in section 3.2, choosing a Thomas-Fermi screening function will tend to overestimate the nuclear stopping power at low energies. Consequently, we must expect to underestimate  $\xi(\epsilon)$ . It appears much more reasonable to choose a nuclear stopping power that agrees better with experimental data. In fact, choosing the universal stopping power from Ziegler et al. which is still closest to Thomas-Fermi, already changes the behavior of  $\xi(\epsilon)$

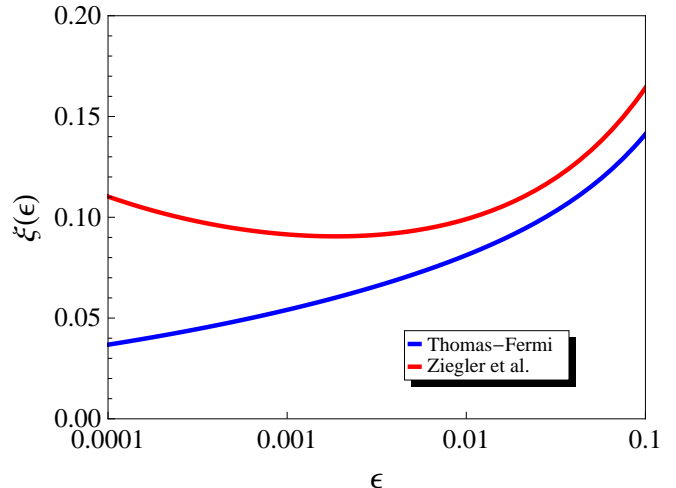


Figure 2: The function  $\xi(\epsilon)$  for different choices of the nuclear stopping power.

considerably (see figure 2). Now,  $\xi(\epsilon)$  is no longer increasing monotonically, but develops a minimum around a few keV, remaining almost constant in most of the region we are interested in.

As we have seen, the uncertainties concerning the fraction of energy deposited in electronic excitations remains quite large. Although Lindhard's theory has been quoted frequently in the context of the effective scintillation yield, it appears difficult to obtain even a general tendency from this theory. We believe that some conclusions drawn from it, especially concerning the energy dependence, depend on quite weak assumptions. Moreover, we will show below, that a much more reasonable agreement with experimental data is achieved for an almost constant  $\xi(\epsilon)$ .

#### 4. Recombination

Now that we have an estimate of the total energy in electronic excitations, we need to determine how this energy is distributed between ionization and scintillation. This distribution depends not only on the number of excited and ionized atoms produced initially, but especially on the recombination rate. Recombination will occur, whenever an electron and an ion produced in a nuclear recoil process approach sufficiently close. The recombination rate should be proportional to the ionization density, which in turn is roughly proportional to the electronic stopping power  $s_e(\epsilon)$ . Consequently, we expect a higher ionization density, and thus a higher recombination rate, at higher recoil energies. Here we can follow closely the Ph.D. thesis of Dahl [28].

As discussed in section 2, after all recoiling atoms have thermalized, we are left with a certain number of excitons, called  $N_{\text{ex}}$ , and a certain number of ionized atoms,  $N_i$ . We expect that a fraction  $r$  of the ionized atoms will

recombine with free electrons, forming excitons that will eventually emit scintillation photons. The number of photons produced should consequently be given by

$$N_{\text{ph}} = N_{\text{ex}} + r \cdot N_{\text{i}} = N_{\text{i}} \left( r + \frac{N_{\text{ex}}}{N_{\text{i}}} \right). \quad (19)$$

We assume that the fraction  $N_{\text{ex}}/N_{\text{i}}$  is energy independent (see [29] for a discussion), although it may depend on the nature of the recoiling particle.<sup>5</sup> The simulations from [28] are in agreement with this assumption. For a discussion on ways to determine  $N_{\text{ex}}/N_{\text{i}}$  experimentally, we refer to [33]. Consequently, an energy dependence can only be introduced by the recombination fraction  $r$ . For later uses, we also define the number of electrons produced,

$$N_{\text{q}} = (1 - r) \cdot N_{\text{i}}. \quad (20)$$

$N_{\text{ex}}$  and  $N_{\text{i}}$  are presently unknown. However, they should both be proportional to  $\kappa(\epsilon)$ , which in turn was determined to be proportional to  $\epsilon\xi(\epsilon)$ . As we kept the constant of proportionality undetermined, we can do the same thing for  $N_{\text{ex}} + N_{\text{i}}$ , writing simply

$$N_{\text{ex}} + N_{\text{i}} = N_{\text{i}} \left( 1 + \frac{N_{\text{ex}}}{N_{\text{i}}} \right) = \beta\epsilon\xi(\epsilon). \quad (21)$$

This allows to calculate  $N_{\text{ex}}$  and  $N_{\text{i}}$  from  $\kappa(\epsilon)$  once we have determined  $N_{\text{ex}}/N_{\text{i}}$  and  $\beta$ . If we also know the recombination fraction  $r(\epsilon)$ , we can then infer  $N_{\text{ph}}$ .

The task is therefore to determine  $N_{\text{ex}}/N_{\text{i}}$  and  $r(\epsilon)$ . It would of course be desirable to derive these quantities from an analytical model. In fact, various theories describing recombination exist (for a review, see [34]). The basic idea is to introduce a critical radius, called Onsager radius, which is defined by

$$\frac{e^2}{r_{\text{c}}} = kT. \quad (22)$$

If the distance between electron and ion is larger than  $r_{\text{c}}$ , thermal fluctuations will prevent recombination, while for smaller distances, recombination will occur. In order to calculate the recombination rate, one needs to describe diffusion processes for electrons and ions. A calculation by Thomas and Imel [35] gives

$$\frac{N_{\text{q}}}{N_{\text{i}}} = 1 - r = \frac{4}{\gamma N_{\text{i}}} \ln \left( 1 + \frac{\gamma N_{\text{i}}}{4} \right), \quad (23)$$

where  $\gamma$  is a free parameter of the theory.<sup>6</sup>

In order to determine  $\gamma$ , Dahl has performed Monte Carlo simulations [28] of nuclear recoils at different recoil

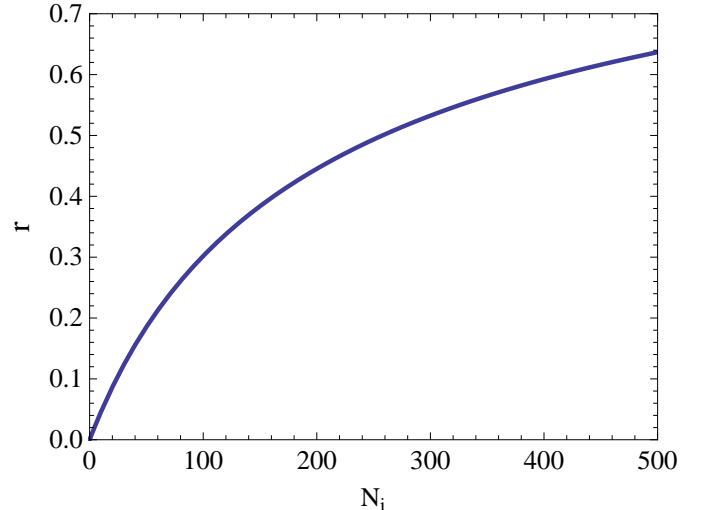


Figure 3: Recombination fraction  $r$  as a function of the number of ionized atoms.

energies. For each recoil energy, the simulation provides  $N_{\text{q}}$ , the number of free electrons remaining after recombination. Now  $\gamma$  can be determined by fitting the theory to the data. Note that  $N_{\text{q}}$  depends not only on  $r$  but also on the total number of ionized atoms produced, so the fit will also determine the previously unknown parameter  $N_{\text{ex}}/N_{\text{i}}$ .

Monte Carlo simulations have been performed for different values of the electric field and show, as expected, a decrease of recombination with increasing field strength. As  $N_{\text{ex}}/N_{\text{i}}$  should not depend on the electric field, only  $\gamma$  is allowed to vary with the electric field strength. We are interested in the limit of zero electric field and consequently take the value of  $\gamma$  for the lowest drift field available, which is 60 V/cm and is much smaller than electric fields usually applied in experiments. The results are

$$\frac{N_{\text{ex}}}{N_{\text{i}}} \approx 0.9, \quad (24)$$

$$\gamma \approx 0.039. \quad (25)$$

The recombination fraction  $r$  is shown in figure 3. As expected, it increases with the total number of produced ions corresponding to higher recoil energies.

## 5. Obtaining the scintillation yield

Having calculated the total energy in electronic excitations and the recombination fraction, we are now able to predict both the ionization and the scintillation yield. However, one free parameter still remains in our theory: the proportionality factor  $\beta$  which we introduced in equation (21). Combining this equation with equation (23), we

<sup>5</sup>For example, we expect  $N_{\text{ex}}/N_{\text{i}}$  to be larger for the collision of two xenon atoms than for electron recoils, because the xenon atoms can temporarily form molecular orbitals that enhance the probability for excitations [30–32].

<sup>6</sup>In fact,  $\gamma$  can be expressed in terms of the mobility of the charge carries,  $\mu$ , the drift velocity,  $v$ , and the typical size of the track,  $a$ :  $\gamma = 4\pi\mu/a^2v$ . However, as these parameters are unknown, we may just as well take  $\gamma$  as the parameter of the theory.

can write

$$N_q(\epsilon) = N_i(\epsilon) \frac{4}{\gamma N_i(\epsilon)} \ln \left( 1 + \frac{\gamma N_i(\epsilon)}{4} \right), \quad (26)$$

$$N_i(\epsilon) = \frac{\beta \xi(\epsilon)}{1 + N_{\text{ex}}/N_i}. \quad (27)$$

$N_q(\epsilon)$  has been measured experimentally (most recently in [6]), so we can determine  $\beta$  from fitting equation (26) to the available data. Instead of  $N_q(\epsilon)$ , one conventionally plots the ionization yield, which is defined as  $Q_y(E_{\text{nr}}) = N_q(E_{\text{nr}})/E_{\text{nr}}$  and measured in  $e^-/\text{keVnr}$ . Of course, it is not possible experimentally to measure the ionization yield at zero electric field, so we must change the value for  $\gamma$  accordingly. We will use the experimental data taken taken at  $E = 1 \text{ kV/cm}$  and take the value  $\gamma = 0.03$  determined by Dahl [28] for  $E = 0.88 \pm 0.04 \text{ kV/cm}$ . Although there is only one free parameter, a reasonable fit can be obtained setting  $\beta = (1.2 \pm 0.1) \cdot 10^5$  (see the red line in figure 4a), which indicate that our description is sufficient.<sup>7</sup>

We are now in the position to predict the relative scintillation efficiency. The value of  $N_{\text{ph}}$  can be obtained directly from  $N_q$  because  $N_q + N_{\text{ph}} = N_{\text{ex}} + N_i = \beta \epsilon \xi(\epsilon)$  and this sum is known once we have determined  $\beta$ . In order to obtain  $\mathcal{L}_{\text{eff}}$ , we need to divide  $N_{\text{ph}}$  by the number of photons produced by the reference electron recoil at 122 keV. This value can be determined from the  $W_{\text{ph}}$  value for xenon, which is the energy that an electron recoil must on average deposit in the detector to produce a scintillation photon. From [36], we take  $W_{\text{ph}} = 21.6 \text{ eV}$  and infer that  $N_{\text{ph}}^{\text{ref}} = 46 \text{ phe/keVee}$ .

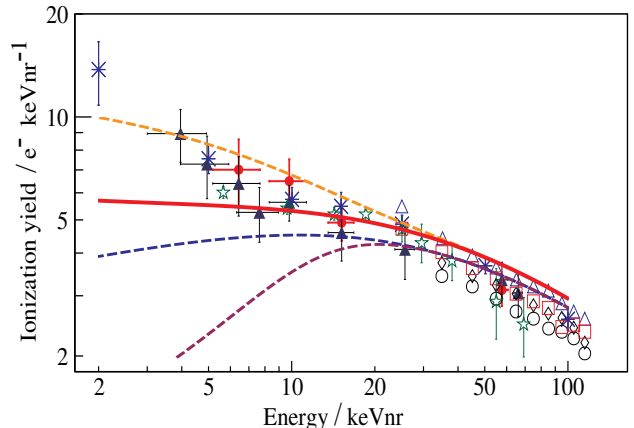
Before giving our result for  $\mathcal{L}_{\text{eff}}$  we need to include one more process, that has been neglected so far. As mentioned in section 2, the number of excitons can be reduced by biexcitonic quenching (see [14, 37, 38]). The idea is that in collisions of two excited atoms, only one scintillation photon is produced. Several authors have suggested a parameterization of this process in terms of Birk's saturation law [38–40]. They introduce an energy dependent quenching factor  $q_{\text{el}}$  given by

$$q_{\text{el}} = \frac{1}{1 + k \cdot s_e(\epsilon)}, \quad (28)$$

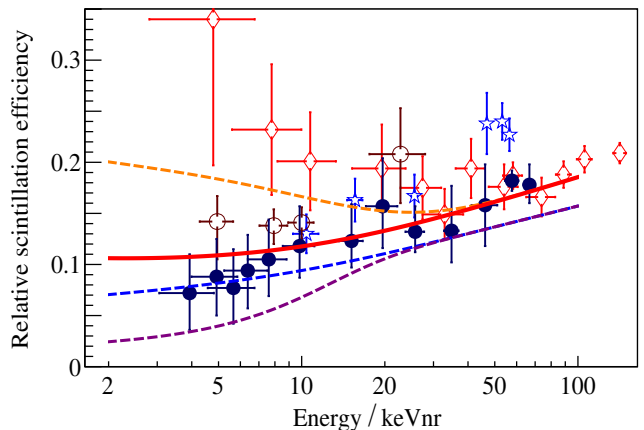
where  $k$  is called Birk's constant and has been determined in [39] to equal  $k = 2.015 \cdot 10^{-3} \text{ g/MeV cm}^2 = 21.4$  in reduced units. The value suggested in [40] is smaller by about 15%. One can see from equation (28) that biexcitonic quenching is very efficient at high recoil energies, when the density of excited atoms is large. However, when only few excited atoms are produced, biexcitonic collisions are rare and cease to reduce the photon yield.

Now we can write down our final result for  $\mathcal{L}_{\text{eff}}$ :

$$\mathcal{L}_{\text{eff}} = \frac{N_{\text{ph}}(E_{\text{nr}})}{E_{\text{nr}} \cdot N_{\text{ph}}^{\text{ref}}} \cdot q_{\text{el}}(E_{\text{nr}}). \quad (29)$$



(a) The ionization yield



(b) The relative scintillation efficiency

Figure 4: Predictions for the ionization yield  $Q_y$  and the relative scintillation efficiency  $\mathcal{L}_{\text{eff}}$  compared to the experimental data presented in [6] (and further references therein). The lines with different colors correspond to different choices of the function  $\xi(\epsilon)$ : The blue line corresponds to the original function  $\xi(\epsilon)$  obtained from Lindhard's theory (nuclear stopping power based on Thomas-Fermi screening). The red line, which we consider as the best description, corresponds to our proposal to modify Lindhard's theory by using the universal nuclear stopping power from Ziegler et al. (see also figure 2). The purple line, has been obtained by assuming a threshold effect at 5 keV that reduces the electronic excitations and consequently acts like a smooth cut-off for  $\xi(\epsilon)$ . The ionization yield becomes clearly inconsistent with data, thus limiting the scintillation efficiency from below. For the orange line, finally, we have included an enhancement of the electronic stopping power at low energies. For all plots we have used  $\beta = 1.2 \cdot 10^5$ . For our prediction of  $Q_y$  we assume an electric field of  $E = 0.88 \pm 0.04 \text{ kV/cm}$ .

<sup>7</sup>The reason why  $\beta$  is so large is that  $\kappa(\epsilon)$  is a reduced energy.

All parameters appearing in this equation have either been measured or were fixed previously. Consequently, we can now plot  $\mathcal{L}_{\text{eff}}$  and compare it with available data (see the red curve in figure 4b). Our model predicts a flat  $\mathcal{L}_{\text{eff}}$  at low recoil energies, giving roughly  $\mathcal{L}_{\text{eff}} = 0.11$  at  $E_{\text{nr}} = 2 \text{ keV}$ . This prediction agrees well with the values measured by Aprile et al. [5]. Also, good agreement in both  $Q_y$  and  $\mathcal{L}_{\text{eff}}$  is found between our results and the results that Sorensen obtained from Monte Carlo simulations of the nuclear recoil band [41].

We would like to emphasize that the Lindhard factor, meaning  $\xi(\epsilon)$ , is still the dominating uncertainty of our model. In fact, we are under the impression, that this uncertainty has often been underestimated previously, since not even the general trend (suppression or enhancement) of electronic excitations at low recoil energies is fully clear. However, the point we would like to emphasize is that different assumptions for the nuclear and electronic stopping powers affect the predictions for both ionization yield and relative scintillation efficiency in a correlated way.

We show in figure 4 different curves corresponding to different assumptions on  $\xi(\epsilon)$  (equivalent to different choices of suppression factor  $F(v/v_0)$  in equation (6)). All choices of  $\xi(\epsilon)$  give predictions for the  $\mathcal{L}_{\text{eff}}$  that are compatible with experimental data. However, if  $\xi(\epsilon)$  decreases with decreasing recoil energy (as one would expect in the presence of threshold effects or Coulomb effects), one cannot account for the increasing ionization yield that we observe experimentally. Our central observation is therefore that any model attempting to explain the scintillation yield of liquid xenon, must at the same time explain the ionization yield. Consequently, a general suppression of electronic excitations at low recoil energies is clearly incompatible with experiments. In contrast, an energy dependent recombination fraction can clearly accommodate (and even predict) the opposing trends seen in scintillation and ionization yield.

Our results rely on the assumption that the ratio  $N_{\text{ex}}/N_i$  does not vary strongly with energy. If we allow for an arbitrary energy dependence of this quantity and simultaneously vary  $\xi(\epsilon)$ , we could obviously fit any measurement for the ionization yield and the relative scintillation efficiency. However, from all available data, such an energy dependence is not expected. Moreover, to suppress scintillation and enhance ionization at low energies,  $N_{\text{ex}}/N_i$  would have to decrease, implying that excitation becomes less likely compared to ionization. Such a behavior would most likely contradict the fact that less energy is required to excite a xenon atom than to ionize it.

## 6. Conclusions

We studied in this paper the behavior of low energy nuclear recoils in liquid xenon which is important for Dark Matter searches. An ab-initio analysis of the problem would require a quantum mechanical calculation of exclusive cross sections in Xe–Xe collisions (elastic, ionizing and

leading to excited atoms) and a Monte Carlo simulation of the propagation of the nuclear recoil and further recombination. The collision analysis should be made for low impact velocities, taking into account the electronic structure of the outer shells of xenon (for example, using Density Functional Theory). Alternatively, these cross sections could be determined in experiments on scattering of individual xenon atoms.

To do so is obviously a formidable task and we pursued therefore a simplified effective framework. Specifically we combined Lindhard’s theory for the initial production of electron excitations in atomic collisions with the well motivated assumption of energy independent partition between ionization and excitation in the underlying collisions. Including an analysis of the recombination processes we obtained *both* the ionization and scintillation yields which show a correlated functional behavior when the stopping powers at low energies are varied. We argued that this correlated behavior allows an interesting consistency check when ionization and scintillation are measured simultaneously. We also argued that this correlation allows to use low recoil energy data for ionization to predict the low recoil energy dependence of scintillation. Using existing low recoil energy data for ionization we showed that it predicts a constant behavior of  $\mathcal{L}_{\text{eff}}$  for low energies and that it allows to exclude the possibility of  $\mathcal{L}_{\text{eff}}$  dropping rapidly to zero below some threshold of 5 keV or more. In the analysis of the first XENON100 data [1], a constant behavior of  $\mathcal{L}_{\text{eff}}$  at low energies was assumed, which led to discussions in the literature about the reliability of the bounds for low WIMP masses. Our study shows that a constant  $\mathcal{L}_{\text{eff}}$  follows from ionization data and this strengthens therefore the low WIMP mass bounds found by the XENON100 collaboration.

## 7. Acknowledgments

F.K. thanks Rafael Lang for helpful comments and discussions. We thank Teresa Marrodan-Undagoitia and Laura Baudis for carefully reading the draft and their useful comments. This work has been supported in part by the DFG Grant No. SFB-TR27 “Neutrinos and Beyond.” F.B. is partially sponsored by the Humboldt Foundation.

## References

- [1] E. Aprile, et al., First Dark Matter Results from the XENON100 Experiment, Phys. Rev. Lett. 105 (2010) 131302. [arXiv:1005.0380](#).
- [2] R. Bernabei, et al., First results from DAMA/LIBRA and the combined results with DAMA/NaI, Eur. Phys. J. C56 (2008) 333–355. [arXiv:0804.2741](#).
- [3] C. E. Aalseth, et al., Results from a Search for Light-Mass Dark Matter with a P-type Point Contact Germanium Detector. [arXiv:1002.4703](#).
- [4] P. Sorensen, et al., The scintillation and ionization yield of liquid xenon for nuclear recoils, Nucl. Instrum. Meth. A601 (2009) 339–346. [arXiv:0807.0459](#).



- [5] E. Aprile, et al., New Measurement of the Relative Scintillation Efficiency of Xenon Nuclear Recoils Below 10 keV, *Phys. Rev. C* 79 (2009) 045807. [arXiv:0810.0274](#).
- [6] A. Manzur, et al., Scintillation efficiency and ionization yield of liquid xenon for mono-energetic nuclear recoils down to 4 keV, *Phys. Rev. C* 81 (2010) 025808. [arXiv:0909.1063](#).
- [7] F. Arneodo, et al., Scintillation efficiency of nuclear recoil in liquid xenon, *Nucl. Instrum. Meth. A* 449 (2000) 147–157.
- [8] D. Akimov, et al., Measurements of scintillation efficiency and pulse-shape for low energy recoils in liquid xenon, *Phys. Lett. B* 524 (2002) 245–251. [arXiv:hep-ex/0106042](#).
- [9] E. Aprile, et al., Scintillation response of liquid xenon to low energy nuclear recoils, *Phys. Rev. D* 72 (2005) 072006. [arXiv:astro-ph/0503621](#).
- [10] V. Chepel, et al., Scintillation efficiency of liquid xenon for nuclear recoils with the energy down to 5 keV, *Astropart. Phys.* 26 (2006) 58–63.
- [11] E. Aprile, et al., Simultaneous Measurement of Ionization and Scintillation from Nuclear Recoils in Liquid Xenon as Target for a Dark Matter Experiment, *Phys. Rev. Lett.* 97 (2006) 081302. [arXiv:astro-ph/0601552](#).
- [12] J. Lindhard, M. Scharff, Energy dissipation by ions in keV region, *Physical Review* 124 (1) (1961) 128.
- [13] S. Ovchinnikov, G. Ogurtsov, J. Macek, Y. Gordeev, Dynamics of ionization in atomic collisions, *Physics Reports-Review Section Of Physics Letters* 389 (3) (2004) 119–159.
- [14] A. Hitachi, T. Doke, A. Mozumder, Luminescence quenching in liquid argon under charged-particle impact - relative scintillation yield at different linear energy transfers, *Physical Review B* 46 (18) (1992) 11463–11470.
- [15] I. Tilinin, Quasi-classical expression for inelastic energy-losses in atomic particle collisions below the bohr velocity, *Physical Review A* 51 (4) (1995) 3058–3065.
- [16] J. Valdes, J. Eckardt, G. Lantschner, N. Arista, Energy-loss of slow protons in solids - deviation from the proportionality with projectile velocity, *Physical Review A* 49 (2) (1994) 1083–1088.
- [17] P. Echenique, R. Nieminen, J. Ashley, R. Ritchie, Nonlinear stopping power of an electron-gas for slow ions, *Physical Review A* 33 (2) (1986) 897–904.
- [18] T. Ferrell, R. Ritchie, Energy-losses by slow ions and atoms to electronic excitation in solids, *Physical Review B* 16 (1) (1977) 115–123.
- [19] H. Winter, J. Juaristi, I. Nagy, A. Arnau, P. Echenique, Energy loss of slow ions in a nonuniform electron gas, *Physical Review B* 67 (24) (2003) 245401.
- [20] O. Firsov, A qualitative interpretation of the mean electron excitation energy in atomic collisions, *Soviet Physics JETP-USSR* 9 (5) (1959) 1076–1080.
- [21] D. J. Ficenec, S. P. Ahlen, A. A. Marin, J. A. Musser, G. Tarle, Observation of electronic excitation by extremely slow protons with applications to the detection of supermassive charged particles, *Phys. Rev. D* 36 (1987) 311–314.
- [22] J. Brenot, D. Dhucq, J. Gauyacq, J. Pommier, V. Sidis, M. Barat, E. Pollack, Collisions between rare-gas atoms at low keV energies - Symmetric Systems, *Physical Review A* 11 (4) (1975) 1245–1266.
- [23] D. Semrad, Coulomb effect and threshold effect in electronic stopping power for slow protons, *Physical Review A* 33 (3) (1986) 1646–1652.
- [24] P. Sigmund, Stopping Of Heavy Ions - A Theoretical Approach, Vol. 204 of Springer Tracts In Modern Physics, Springer-Verlag Berlin, 2004, pp. 1–5.
- [25] K. Winterbon, P. Sigmund, J. Sanders, Spatial distribution of energy deposited by atomic particles in elastic collisions, *Kongelige Danske Videnskabernes Selskab, Matematisk-Fysiske Meddelelser* 37 (14) (1970) 5–61.
- [26] J. Ziegler, J. Biersack, U. Littmark, Stopping and range of ions in solids, 1985.
- [27] J. Lindhard, V. Nielsen, M. Scharff, P. Thomsen, Integral equations governing radiation effects, *Mat. Fys. Medd. Dan. Vid. Selsk.* 33 (10) (1963) 1.
- [28] C. Dahl, The physics of background discrimination in liquid xenon, and first results from Xenon10 in the hunt for WIMP dark matter, Ph.D. thesis, Princeton University (2009).
- [29] R. Platzman, Total ionization in gases by high-energy particles - an appraisal of our understanding, *International Journal Of Applied Radiation And Isotopes* 10 (1961) 116.
- [30] U. Fano, W. Lichten, Interpretation of  $\text{Ar}^+ - \text{Ar}$  Collisions at 50 KeV, *Phys. Rev. Lett.* 14 (1965) 627–629.
- [31] R. Spicuzza, Q. Kessel, Ionization due to multiple n-shell and m-shell excitation in penetrating collisions of 0.15-1.20 MeV  $\text{Xe}^+$  with Xe, *Physical Review A* 14 (2) (1976) 630–637.
- [32] M. Kimura, N. Lane, The low-energy, heavy-particle collisions - a close coupling treatment, *Advances In Atomic Molecular And Optical Physics* 26 (1989) 79–160.
- [33] A. Manalaysay, Response of liquid xenon to low-energy ionizing radiation and its use in the XENON10 Dark Matter search, Ph.D. thesis, University of Zurich (2010).
- [34] S. Amoruso, et al., Study of electron recombination in liquid argon with the ICARUS TPC, *Nucl. Instrum. Meth. A* 523 (2004) 275–286.
- [35] J. Thomas, D. A. Imel, Recombination of electron-ion pairs in liquid argon and liquid xenon, *Physical Review A* 36 (1987) 614–616.
- [36] E. Aprile, T. Doke, Liquid xenon detectors for particle physics and astrophysics, *Reviews of Modern Physics* 82 (2010) 2053–2097. [arXiv:0910.4956](#).
- [37] A. Hitachi, Quenching factor and electronic LET in a gas at low energy, *J. Phys. Conf. Ser.* 65 (2007) 012013.
- [38] A. Hitachi, Properties of liquid xenon scintillation for dark matter searches, *Astropart. Phys.* 24 (2005) 247–256.
- [39] D.-M. Mei, Z.-B. Yin, L. Stonehill, A. Hime, A Model of Nuclear Recoil Scintillation Efficiency in Noble Liquids, *Astropart. Phys.* 30 (2008) 12–17. [arXiv:0712.2470](#).
- [40] V. Tretyak, Semi-empirical calculation of quenching factors for ions in scintillators, *Astropart. Phys.* 33 (2010) 40–53. [arXiv:0911.3041](#).
- [41] P. Sorensen, A coherent understanding of low-energy nuclear recoils in liquid xenon. [arXiv:1007.3549](#).